# Polymer Chemistry



**PAPER** 

View Article Online
View Journal | View Issue



**Cite this:** *Polym. Chem.*, 2023, **14**, 1915

# Solvent-induced competing processes in polycarbonate degradation: depolymerization, chain scission, and branching/crosslinking†

Mengqi Sun, D<sup>a</sup> Zhen Xu, Nuwayo Eric Munyaneza, Yue Zhang, Carlos Posada and Guoliang Liu +A,b,c

Poly(bisphenol A carbonate) (PC) is a massively produced engineering plastic and requires innovative recycling methods at its end of life. In this work, we investigate the chemical degradation of PC in dimethyl-formamide (DMF) and dimethyl sulfoxide (DMSO), catalyzed by copper sulfide nanoparticles (CuS NPs). In DMF, PC is degraded to bisphenol A (BPA) *via* hydrolytic decomposition with an appreciable yield of ~80%. In contrast, the degradation of PC in DMSO yields oligomeric or branched/crosslinked PC, possibly due to radical-assisted chain cleavage. Temperature and solution heterogeneity are two parameters that dictate the competition between chain scission and branching/crosslinking. The different degradation behaviors of PC in DMF and DMSO highlight the importance of solvents in polymer degradation, which can lead to different pathways of hydrolytic depolymerization or radical-assisted chain scission, branching, and crosslinking. This work provides new insight into the recycling of plastic waste and offers new avenues to induce polymer branching/crosslinking.

Received 17th December 2022, Accepted 17th March 2023 DOI: 10.1039/d2py01572b

rsc.li/polymers

# Introduction

End-of-life plastics pose environmental challenges and spur extensive efforts in recycling. Poly(bisphenol A carbonate) (PC), massively produced at 4.5 million tons annually, is one of the most produced engineering plastics. It has wide applications in electronics, construction, automotive systems, and aircraft owing to its excellent mechanical, thermal, and optical properties. The enormous global production has led to an urgent need for effective recycling. Among various recycling approaches, chemical recycling holds great promise because it can degrade polymers into easily processable building blocks or valuable chemicals. Hydrolysis, Hydrolysis, thermolysis, alcoholysis, aminolysis, and hydrogenation are among the most extensively investigated approaches.

Hydrolysis of polycarbonates could date back to 1962.<sup>32</sup> The hydrolytic reaction with hydroxide ions converts PC to bisphenol A (BPA) and CO<sub>2</sub>.<sup>32,34,38</sup> The resulting BPA monomer can

be used as a chemical feedstock, enabling the conversion of

Besides hydrolysis, radical-assisted degradation is another effective chemical degradation approach. Radicals are often generated by heat or light. UV photolysis<sup>51,52</sup> is a common method to generate free radicals for polymer degradation. The high-energy photons cleave the polymer chains and leave radicals in the backbone, which lead to β-chain scission and yield products with smaller molecular weights. The radicals can undergo propagation and transfer before recombination to terminate the reaction. 53-60 Since the short-lived radicals can potentially induce polymer branching or crosslinking, there exists a competition between chain scission and chain branching/crosslinking. Only the former leads to polymer degradation to small molecules; the latter can produce high-molecularweight polymers and possibly be used for polymer modification. For instance, Graebling used thiuram disulfide compounds to suppress β-scission and facilitate branching (grafting) of polypropylene (PP) in the reactive extrusion process.<sup>61</sup> Borsig et al. blended PP with polyethylene (PE) as a way to

PC to other engineering plastics.<sup>36</sup> Inorganic catalysts have been used to improve the degradation efficiency because they coordinate with the carbonyl group to enhance its electrophilicity.<sup>31,35,37,39</sup> However, due to the hydrophobic nature of PC, the industrial hydrolysis process requires high temperature steam to ensure phase compatibility.<sup>6,34,40</sup> Judiciously selected solvents can potentially circumvent the energy-intensive approaches and maintain phase compatibility.

<sup>&</sup>lt;sup>a</sup>Department of Chemistry, Virginia Tech, Blacksburg, Virginia 24061, USA. E-mail: gliu1@vt.edu

 $<sup>^</sup>bDepartment$  of Chemical Engineering, Virginia Tech, Blacksburg, Virginia 24061, USA

<sup>&</sup>lt;sup>c</sup>Department of Materials Science and Engineering, Virginia Tech, Blacksburg, Virginia 24061, USA

<sup>†</sup>Electronic supplementary information (ESI) available: Additional EDS, PXRD, GPC, GC-MS, NMR, and DSC results. See DOI: https://doi.org/10.1039/d2py01572b

**Polymer Chemistry** Paper

reduce β-scission and achieved crosslinked PP/PE polymer blends. 62 François-Heude et al. studied the kinetics of photothermal and thermal oxidation on isotactic polypropylene (iPP) films. 63 They found that with additional hydroperoxide photolysis, chain scission dominated over branching or crosslinking under photothermal conditions. 63 Triacca et al. designed both experimental and computational studies on the radical-assisted chain scission of PP and used a low concentration of a radical initiator to avoid the undesired crosslinking. 64 Ahn et al. computationally investigated the radical reactions in PE radio-oxidation and found that the final products were mainly produced by crosslinking, chain scission, and termination through alcohol and ketone groups. 65 Thus, understanding the competition between polymer chain scission and branching/crosslinking is critical in designing polymer degradation processes.

Herein, we have investigated the degradation of PC in two solvents of dimethylformamide (DMF) and dimethyl sulfoxide (DMSO) (Fig. 1). PC underwent hydrolytic depolymerization to produce BPA in DMF and radical-assisted degradation to yield oligomers and branched/crosslinked polymers in DMSO. DMSO can serve as an effective source to generate various radical species. 66-74 To facilitate the radical generation, 75-79 copper sulfide (CuS) nanoparticles (NPs) were synthesized and used as catalysts. The DMSO-generated radicals participated in the chain cleavage reaction, leading to competing processes of oligomerization and branching/crosslinking depending on the reaction temperature and solution heterogeneity.

# Experimental

#### **Materials**

Bisphenol A-polycarbonate (BPA-PC) was purchased from Lexan (LEXAN<sup>TM</sup> 123R resin). Dimethyl sulfoxide (DMSO, VWR), anhydrous DMSO (anhydrous 99.9%, Sigma-Aldrich), N-dimethylformamide (DMF, Sigma-Aldrich), anhydrous DMF (anhydrous 99.8%, packaged under Argon, Sigma-Aldrich), hydrogen peroxide (H2O2, 30 wt% in water, ACS reagent grade, Sigma-Aldrich), chloroform (HPLC, Thermo Fisher Scientific),

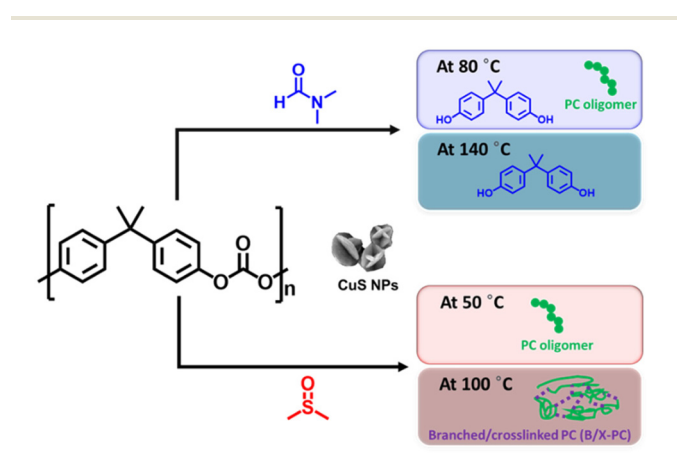


Fig. 1 Scheme of PC degradation in DMF and DMSO.

copper nitrate trihydrate (Cu(NO<sub>3</sub>)<sub>2</sub>·3H<sub>2</sub>O<sub>4</sub>, 98%, Sigma-Aldrich), thiourea (ReagentPlus, >99%, Sigma-Aldrich), ethylene glycol (general lab grade, Thermo Fisher Scientific), polyvinylpyrrolidone (PVP,  $M_{\rm w}$  = 29 000 Da, Sigma-Aldrich), ethanol (VWR), methanol (VWR), and deuterated chloroform (CDCl<sub>3</sub>, 99.8%, Cambridge Isotope Laboratories, Inc.) were used as received.

#### Characterization

Number average molecular weight  $(M_n)$  of polymers was measured using an EcoSEC HLC-8320GPC Size-exclusion Chromatography (SEC) system equipped with two TSKgel SuperHM-H columns, a refractive index detector, and a multiangle light scattering detector (SEC-MALS) at 50 °C. The mobile phase for the SEC-MALS was DMF containing 0.05 M LiBr at a flow rate of 0.5 mL min<sup>-1</sup>. The specific refractive index increment (dn/dc) of PC in DMF was determined to be  $0.14 \text{ mL g}^{-1}$ . Fourier transform infrared spectroscopy (FTIR) was performed at room temperature using a PerkinElmer ATR-FTIR (model Spectrum 100) in the range of 4000-400 cm<sup>-1</sup> with 128 scans and a resolution of 4.0 cm<sup>-1</sup>. Gas chromatography-mass spectroscopy (GC-MS) was performed on a 6890 GC with a 5973 Mass Selective Detector (MSD) from Agilent. The MS Wiley library was used to identify the peaks. Separations were performed using the same GC column under the same operating conditions. The MSD transfer line temperature was 260 °C. Chloroform was added as a reference for quantification analysis. Carbon-13 nuclear magnetic resonance (13C NMR) spectroscopy was performed on a Varian Unity 500 spectrometer at 499.98 MHz in CDCl<sub>3</sub>. Scanning Electron Microscopy (SEM, JEOL IT-500HR) at an accelerating voltage of 2 kV and a working distance of ~5 mm was performed to characterize the morphology of the synthesized NPs. Energy-dispersive X-ray Spectroscopy (EDS) was used to analyze the composition of the NPs. Powder X-ray diffraction (PXRD, Rigaku MiniFlex 300/600, Cu Kα = 1.5405 Å) was used to obtain crystallographic information on the synthesized CuS NPs. Differential Scanning Calorimetry (DSC) was performed between 20 °C and 300 °C at a heating/cooling rate of 10 °C min<sup>-1</sup> under a nitrogen stream of 50 mL min<sup>-1</sup> on a Discovery DSC2500 (TA Instruments).

#### Synthesis of CuS NPs

First, two precursor solutions of 0.1 M copper nitrate trihydrate (Cu(NO<sub>3</sub>)<sub>2</sub>·3H<sub>2</sub>O) and 0.1 M thiourea were prepared in ethylene glycol (EG). In a round-bottom flask (RBF), 0.2 g of PVP was dissolved in 12 mL of EG. Then, 1 mL of 0.1 M Cu (NO<sub>3</sub>)<sub>2</sub>·3H<sub>2</sub>O and 2 mL of 0.1 M thiourea EG solution were added to the RBF. The reaction mixture was heated to its boiling point of 197 °C and was kept boiling for 40 min. The solution color changed from colorless to light yellow and then to dark green. The synthesized CuS NPs were collected after five cycles of centrifugation and redispersion in ethanol. In the last cycle, the CuS NPs were dispersed in 10 mL ethanol and then stored in a refrigerator.

Polymer Chemistry Paper

#### Degradation of PC in DMF

To conduct PC degradation in DMF, PC (50 mg) was first dissolved in DMF (5 mL). From the ethanol solution of CuS NPs, 600  $\mu$ L was taken and centrifuged in DMF three times. After the last centrifugation, CuS NPs (estimated to be 3.8 mg) were dispersed in the PC/DMF solution. The mixture was under magnetic stirring of 300 revolutions per minute (rpm) and heated at 80 °C or 140 °C for varying reaction times in the range of 3 to 72 h to initiate the degradation reaction. After the reaction, CuS NPs were separated from the solution via centrifugation before analysis. To analyze the macromolecular PC oligomer products, the oligomers were collected via precipitation by methanol. The reaction in anhydrous DMF was similar, except that a Schlenk tube was used as the reaction vessel, and nitrogen purging was performed five times to remove moisture.

#### Homogeneous degradation of PC in DMSO

To conduct PC homogeneous degradation in DMSO, PC (50 mg) was added to DMSO (5 mL). After 8 h of magnetic stirring at 300 rpm and 50 °C, PC was only partially dissolved. The undissolved PC was collected *via* centrifugation, rinsed with methanol, dried in an oven, and weighed and its weight was  $\sim \!\! 38.9$  mg. The dissolved PC was determined to be  $\sim \!\! 11.1$  mg (Table S2†). Similar to the degradation of PC in DMF, 600  $\mu L$  of the CuS/ethanol solution was taken and centrifuged in DMSO three times. After the last centrifugation, CuS NPs were dispersed in the PC in DMSO solution. The mixture was under magnetic stirring of 300 rpm and heated at 50 °C or 100 °C for varying reaction times in the range of 12 to 72 h. After the reaction, CuS NPs were removed *via* centrifugation. PC oligomers were collected *via* precipitation by methanol.

#### Heterogeneous reaction of PC in DMSO

Compared to the homogeneous degradation of PC in DMSO, a heterogeneous reaction of PC in DMSO was conducted without removing the undissolved PC. PC (50 mg) was added to DMSO (5 mL). In a centrifuge tube, 600 µL of the CuS/ethanol solution was centrifuged in DMSO three times. After the last centrifugation step, CuS NPs were dispersed in the PC/DMSO solution. The solution was under magnetic stirring of 300 rpm and heated at 50 °C or 100 °C for varying reaction times in the range of 6 to 30 h. After the reaction, CuS NPs were removed *via* centrifugation. The reacted PC polymers were collected *via* centrifugation and precipitation by methanol.

## Results and discussion

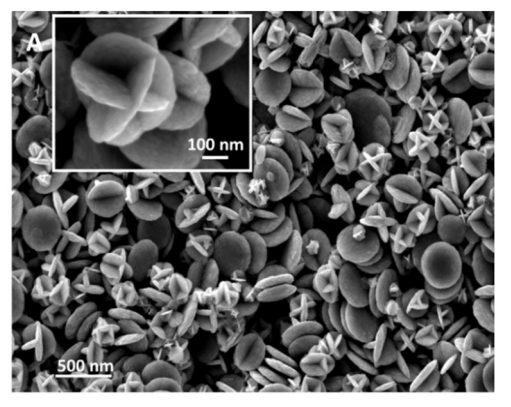
#### Synthesis and characterization of CuS NPs

We have used CuS NPs as the catalyst for PC degradation. CuS was synthesized from precursors of copper nitrate and thiourea in ethylene glycol (EG) at 197 °C using polyvinyl pyridine (PVP) as a surfactant, similar to previous reports. <sup>80–83</sup> The synthesized CuS NPs adopted a hexagonal close-packed (hcp) crystal structure and appeared as anisotropic nanoplates. The nanoplates clustered together and formed three-dimensional

"flower-like" structures (Fig. 2A). Powder X-ray diffraction (PXRD) (Fig. 2B) confirmed that the CuS NPs were hcp covellite, in agreement with the standard, JCPDS no. 06-464. Compositional analysis using energy-dispersive X-ray spectroscopy (EDS) showed an atomic ratio of Cu-to-S close to 1:1 (Fig. S1†). Particle size analysis showed an average diameter of ~304 nm (Fig. S2†).

#### PC depolymerization in DMF

Based on the calculated Flory–Huggins interaction parameters (ESI $^{\dagger}$ ), PC has a higher solubility in DMF than in DMSO, as confirmed by the solubility test (Table S1 and Fig. S3 $^{\dagger}$ ). The different solubilities can lead to different degradation processes of PC in the two solvents. To compare the degradation behaviors in DMF and DMSO, PC degradation was first conducted in DMF at 80 °C and 140 °C. The evolution of PC molecular weight was monitored using gel permeation chromatography (GPC), showing a continuous decline of molecular weight with time (Fig. 3A). Only partial degradation was achieved at 80 °C, and a macromolecular component could still be detected by GPC. As evidenced by the decline rate of  $M_n$  (Fig. 3B), the degradation at 140 °C was much faster, and it reached completion after 24 h without any macromolecular signals detectable by GPC.



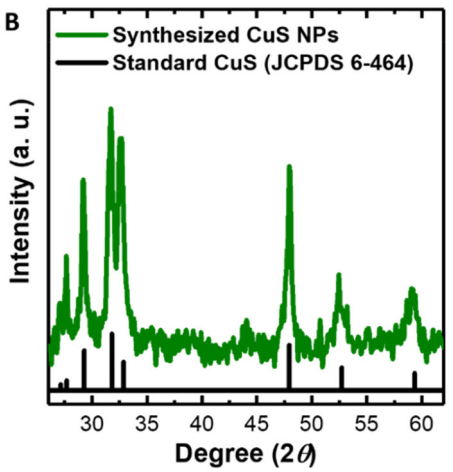


**Fig. 2** Characterization of CuS NPs. (A) SEM images of CuS NPs. (B) PXRD pattern of CuS NPs compared with the standard (JCPDS 6-464).

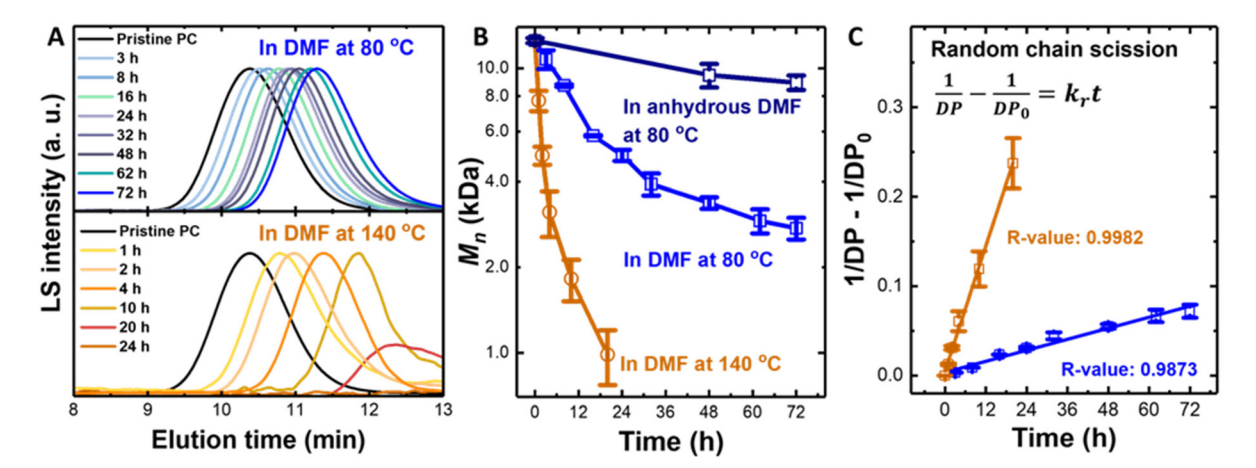


Fig. 3 Reaction kinetics of PC degradation in DMF. (A) GPC traces and (B)  $M_n$  evolution of PC degradation in DMF at 80 °C and 140 °C and in anhydrous DMF at 80 °C. (C) PC degradation at 80 °C and 140 °C exhibits a random chain scission mechanism based on the kinetic fitting. Fitting equation and R-values are shown.

To evaluate the importance of catalysts, control experiments of PC degradation without CuS NPs were conducted. PC showed almost no degradation after 72 h at 80 °C and a slight decrease in  $M_{\rm p}$  after 24 h at 140 °C (Fig. S4†). This observation agrees with previous reports, where inorganic catalysts assisted in the hydrolysis of carbonates by coordinating with the carbonyl oxygen to enhance its electropositive character, thus making it susceptible to nucleophilic attack. 33,37,39 The proposed catalytic role of CuS NPs was supported by additional control experiments. Carbon-13 nuclear magnetic resonance (13C-NMR) spectroscopy was used to analyze the chemical structures of PC (Fig. S5†). After PC and CuS NPs were added to DMF or DMSO, we observed a slight downfield shift and therefore deshielding of the carbonyl peak, indicating a slightly lower electron density around carbonyl carbon. This slight deshielding is possibly due to the coordination of carbonyl with CuS NPs.

The degraded compounds in DMF were determined by gas chromatography-mass spectroscopy (GC-MS). BPA was recovered and confirmed by MS (Fig. 4). Quantitative analysis showed BPA yields of  $\sim$ 48.7 wt% at 80 °C and  $\sim$ 80.3 wt% at 140 °C. PC oligomers were collected and determined to be  $\sim$ 39.4 wt% for degradation in DMF after 72 h at 80 °C, in agreement with the GPC characterization. These results suggested that the degradation of PC in DMF involves the cleavage of carbonate and the BPA yield increased with reaction temperature. A small amount of side products was also detected (Fig. S6†).

The depolymerization of PC in DMF likely follows the hydrolytic decomposition route. Due to the nucleophilicity  $^{84,85}$  and tendency to be protonated,  $^{86}$  DMF can be partially protonated by water to release hydroxide ions, which participate in the nucleophilic reaction with the carbonate group in PC. About 3.7 wt% of residual water was found in DMF (Fig. S7†). During the process, carbon dioxide was released and collected (Fig. S8†). In the absence of water (*i.e.*, in anhydrous DMF), the  $M_{\rm n}$  decline rate of PC was significantly slower (Fig. 3B and Fig. S9†). About 89.1 wt% of the PC degradation products in

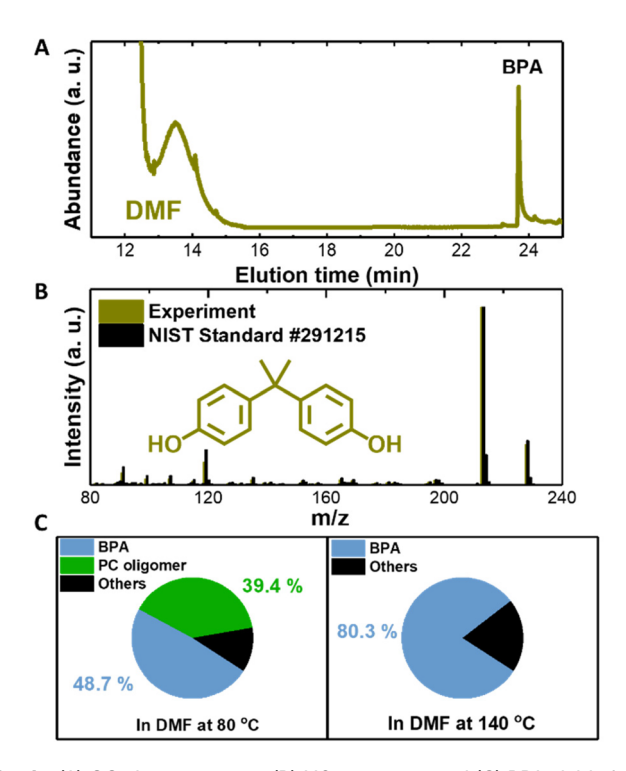


Fig. 4 (A) GC chromatogram, (B) MS spectrum, and (C) BPA yields from the degradation of PC in DMF. PC oligomers were present after degradation in DMF at 80  $^{\circ}$ C for 72 h but absent at 140  $^{\circ}$ C for 24 h.

anhydrous DMF were oligomers, with minor side products of BPA and carbonates due to the lack of hydroxide ions for carbonate cleavage (Fig. S10†).

#### PC oligomerization and branching/crosslinking in DMSO

In addition to DMF, PC degradation was conducted in DMSO. Because PC has low solubility in DMSO, we first established a homogeneous reaction in DMSO by removing the undissolved PC (Table S2†). Meanwhile, degradation also proceeds hetero-

geneously without removing the undissolved PC. The degradation kinetics indicated strong dependence on the reaction temperature and homogeneity. In a homogeneous solution at 50 °C, PC underwent oligomerization, and  $M_{\rm n}$  decreased continuously as the reaction progressed (Fig. 5A and the red curve in Fig. 5B). However, at 100 °C and under heterogeneous conditions, GPC traces displayed bimodal patterns. A new GPC peak at a shorter elution time emerged and intensified over time, corresponding to an increased  $M_{\rm p}$  by about 100-fold (Fig. 5A and the purple curve in Fig. 5B), likely due to chain branching or crosslinking (B/X-PC). To estimate the degree of branching/crosslinking after the heterogeneous reaction of PC in DMSO, B/X-PC was fully dissolved in tetrahydrofuran (THF) and analyzed using GPC. Based on the GPC traces (Fig. S11†) and comparing the intensities of the two peaks of branched/ crosslinked PC and pristine PC, a substantial amount of the polymer chains was branched/crosslinked.

To further probe the effect of reaction temperature and homogeneity, we conducted PC degradation under two more conditions: homogeneous reaction at 100 °C and heterogeneous reaction at 50 °C. The  $M_{\rm n}$  evolution of both degradation reactions was "V-shaped" (Fig. 5B, green and pink curves), suggesting PC chain oligomerization and branching/crosslinking. For the homogeneous reaction at 100 °C, the initial rate of oligomerization was faster than that of the homogeneous reaction at 50 °C (green and red curves). However, the peak position of the GPC trace after the 48 h reaction (Fig. S12A†) downshifted to a shorter elution time, and another GPC peak appeared at a shorter elution time. The increasing molecular weight implied that polymer branching/crosslinking occurred and increased over time, which induced the formation of branched/crosslinked PC.

Similarly, for the heterogenous reaction at 50 °C (pink curve), an initial slow oligomerization was followed by the

downshifting of the GPC trace and the appearance of a new peak at a lower elution time (Fig. S12B†). The new GPC peak of the heterogeneous reaction at 50 °C has a smaller intensity and width than that of the homogeneous reaction at 100 °C, implying a lower degree of branching/crosslinking. It is reported that DMSO can generate radicals upon interacting with reactive oxygen species (ROS) or in the presence of a base. 66-74 The radical generation rate depends on temperature following the Arrhenius equation. Upon lowering the reaction temperature from 100 °C to 50 °C, the concentration of radicals decreased, and the number of polymer chain branching/ crosslinking events decreased. Hence, the impact of reaction temperature and heterogeneity on the PC degradation behaviors in DMSO can be summarized as follows: high reaction temperature favors both chain scission and branching/crosslinking, and heterogeneity favors the branching/crosslinking only.

To investigate the role of CuS NPs, control experiments without CuS NPs were conducted. PC underwent chain cleavage without CuS NPs, but the reaction rates were drastically slower (Fig. S13†). Only PC oligomerization was observed in the homogeneous reaction at 50 °C, and branching/cross-linking occurred in the heterogeneous reaction at 100 °C. These reactions can be ascribed to the strong tendency of DMSO to generate radicals, <sup>66–74</sup> even in the absence of CuS NP catalysts. However, CuS NPs significantly boosted the radical generation of DMSO through their peroxidase-like behavior to catalyze the generation of ROS, <sup>75–79</sup> which can be intercepted by DMSO to generate other radicals. <sup>66–74</sup> Consequently, PC chain oligomerization and branching/crosslinking were facilitated.

The role of an external initiator was explored by adding hydrogen peroxide  $(H_2O_2)$  as a hydroxyl radical (a type of ROS) initiator (Fig. S14†). With  $H_2O_2$ , PC branching/crosslinking

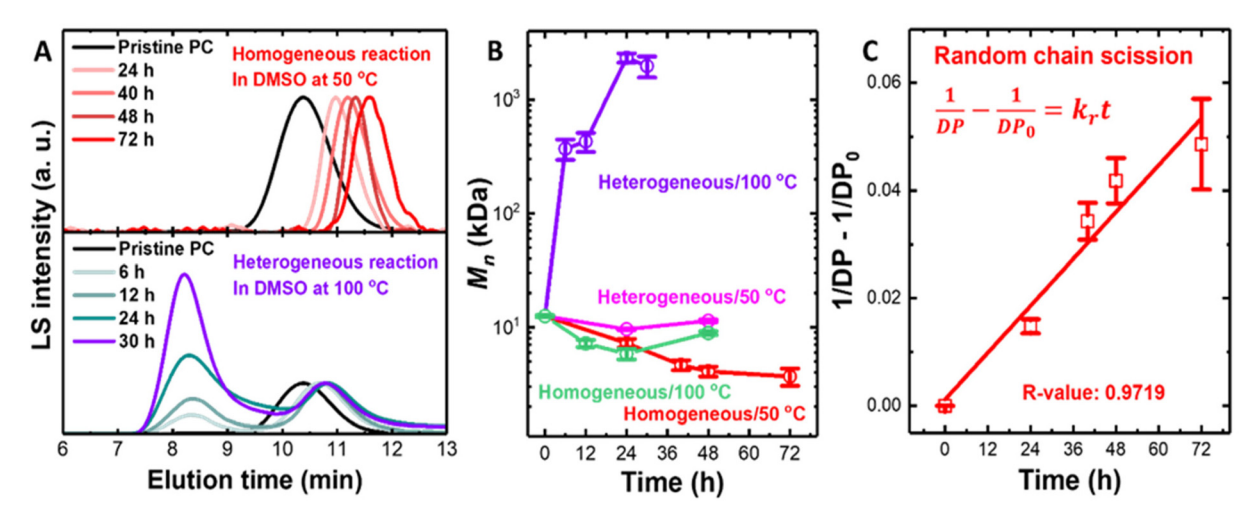


Fig. 5 Reaction kinetics of PC degradation in DMSO. (A) GPC traces of PC homogeneous degradation in DMSO at 50 °C and heterogeneous degradation at 100 °C. (B)  $M_n$  Evolution of PC homogeneous and heterogeneous degradation in DMSO at 50 °C and 100 °C. Only homogeneous PC degradation in DMSO at 50 °C showed continuous oligomerization without crosslinking. (C) Kinetic fitting of homogeneous PC degradation in DMSO at 50 °C exhibited a random chain scission mechanism.

was augmented, shifting the competition between chain oligomerization and branching/crosslinking towards the latter. These results consolidated the hypothesis that excessively concentrated radicals could branch/crosslink the polymers rather than degrading them. To pinpoint the chain-scission pathway, we have considered PC degradation in DMF and DMSO following the random chain-scission mechanism or the chain-end scission mechanism.<sup>87</sup> If the degradation follows the random chain scission pathway, the degree of polymerization (DP) should follow the relationship,<sup>87</sup>

$$\frac{1}{\mathrm{DP}} - \frac{1}{\mathrm{DP}_0} = k_{\mathrm{r}}t\tag{1}$$

where  $k_{\rm r}$  is the reaction constant, t is the reaction time, and DP<sub>0</sub> is the initial degree of polymerization. If the degradation proceeds according to the chain-end scission mechanism, DP should follow the following relationship,<sup>87</sup>

$$DP_0 - DP = k_e t \tag{2}$$

where  $k_{\rm e}$  is the reaction constant. Based on the linear fitting of  $\frac{1}{\rm DP}$  with respect to time (Fig. 3C and 5C), the degradation of PC in both DMF and DMSO adopted the random chain scission pathway. The poor fitting of DP with respect to time ruled out the chain-end scission mechanism (Fig. S15†).

To analyze the backbone structures of PC after oligomerization and branching/crosslinking in DMSO, <sup>13</sup>C-NMR was conducted on B/X PC (after heterogeneous reaction at 100 °C), PC oligomers (after homogeneous reaction at 50 °C) and pristine PC (Fig. S16†). While B/X PC and PC oligomers largely assumed the BPA-based backbone structures of pristine PC, B/X PC showed a new peak at 40.8 ppm. The formation of this new alkyl carbon might suggest that the branching/crosslinking occurred at the methyl groups in the backbone of PC.

The chemical structural information of B/X-PC was further evaluated by Fourier-transform infrared spectroscopy (FTIR). After 30 h of heterogeneous degradation reaction at 100 °C, the resulting B/X-PC exhibited several features (Fig. 6A): broadening of C=O stretching at 1800–1760 cm<sup>-1</sup> and the appearance of C=C stretching at 1660–1640 cm<sup>-1</sup> and O-H stretching at 3600–3000 cm<sup>-1</sup>. The formation of alcohol and carbonyl groups could be attributed to the oxidation of carbon-centered

radicals. On the one hand, the C=C double bond could result from a disproportionation reaction between two terminating carbon-centered radicals. On the other hand, two terminating carbon-centered radicals may combine, enabling the branching and crosslinking of PC chains.

The PC chain branching/crosslinking endowed the polymers with solvent resistance (Fig. 6B). A solubility test of B/X-PC and pristine PC showed that pristine PC was fully soluble in DMF, but B/X-PC could only be partially swollen by DMF. Despite the slightly different solubilities, the thermal properties of B/X-PC were much like those of pristine PC, as characterized by differential scanning calorimetry (DSC) (Fig. S17†).

The different chemical products and branching/crosslinking behaviors confirmed that PC degradation in DMSO was dramatically different from that in DMF. There are three notable differences in the roles of DMSO and DMF in the degradation reactions: (1) PC has a higher solubility in DMF than in DMSO (Table S1 and Fig. S3†); (2) DMF acts as a base promoter to partially dissociate water and facilitate the hydrolysis of PC via a nucleophilic reaction; 84-86 (3) DMSO acts as a radical source and supplies reactive radicals to participate in PC degradation,66-74 but DMF has limited ability to act as a radical source;66 These differences in the chemical and physical properties of solvents result in different degradation behaviors of PC, which are hydrolysis in DMF and radical-assisted degradation in DMSO with competing processes of chain scission and branching/crosslinking. The branched and crosslinked PC showed modified chemical and physical properties, such as new functionalities and lower solubility in DMF. Effective degradation of another BPA-based engineering plastic polyetherimide (PEI) in DMSO was also observed as a proof-of-concept of radical-assisted polymer degradation in DMSO (Fig. S18†).

## Conclusions

Here we have reported the degradation of PC in two solvents of DMF and DMSO. Catalyzed by CuS NPs, PC was depolymerized to BPA in DMF *via* hydrolysis. In DMSO, however, PC underwent radical-assisted chain cleavage to form PC oligomers and/or branched/crosslinked PC (B/X PC). The reaction temp-

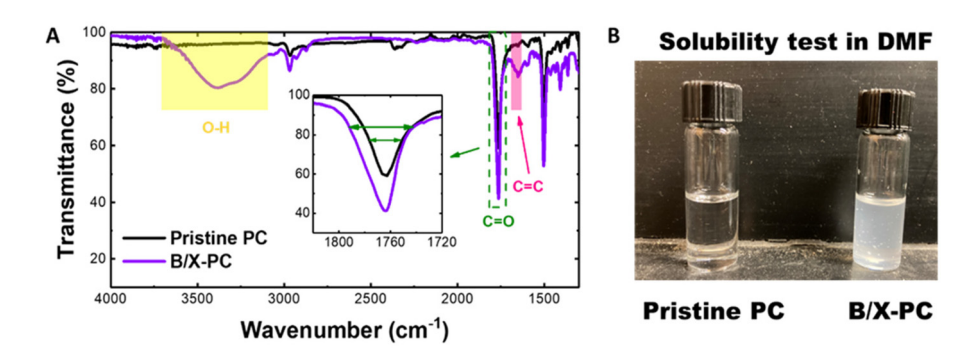


Fig. 6 The branching/crosslinking of PC (B/X-PC) upon heterogeneous reaction in DMSO at 100 °C. (A) FTIR spectra and (B) solubility test of pristine PC and B/X-PC in DMF.

erature and heterogeneity played critical roles in the competition between chain oligomerization and branching/crosslinking: elevated temperatures favor both chain oligomerization and branching/crosslinking because of faster radical generation, while heterogeneous conditions favor only chain branching/crosslinking due to strong chain entanglement. The branched/crosslinked PC after degradation in DMSO exhibited reduced solubility in DMF. Insights drawn from the PC degradation in DMF and DMSO can guide future plastic waste recycling, especially in the selection of solvents for degradation. The interesting competition of chain scission and crosslinking/branching induced by radicals can possibly lead to the development of innovative plastic recycling methods. Mechanistic studies of radicals in polymer degradation are currently underway, including detection of radical species, mechanistic pathways, and degradation of other polymers.

# Conflicts of interest

There are no conflicts to declare.

# Acknowledgements

This work is supported by NSF DMR-1752611 through the CAREER Award, NSF Division of Civil, Mechanical, and Manufacturing Innovation (CMMI), and the American Chemical Society Petroleum Research Foundation through the Doctoral New Investigator (DNI) Award. We acknowledge the use of the Nanoscale Characterization and Fabrication Laboratory (NCFL), facilities of the Department of Chemistry at Virginia Tech, and Dr Mehdi Ashraf-Khorassani for his help in GC-MS instrumentation.

#### References

- 1 A. Chamas, H. Moon, J. J. Zheng, Y. Qiu, T. Tabassum, J. H. Jang, M. Abu-Omar, S. L. Scott and S. Suh, *ACS Sustainable Chem. Eng.*, 2020, **8**, 3494–3511.
- 2 D. K. A. Barnes, F. Galgani, R. C. Thompson and M. Barlaz, Philos. Trans. R. Soc., 2009, 364, 1985–1998.
- 3 P. Dwivedi, P. K. Mishra, M. K. Mondal and N. Srivastava, *Heliyon*, 2019, 5, e02198.
- 4 J. R. Jambeck, R. Geyer, C. Wilcox, T. R. Siegler, M. Perryman, A. Andrady, R. Narayan and K. L. Law, *Science*, 2015, 347, 768–771.
- 5 B. M. Weckhuysen, Science, 2020, 370, 400-401.
- 6 J. G. Kim, Polym. Chem., 2020, 11, 4830-4849.
- 7 Covestro, Polycarbonates demand worldwide from 2011 to 2021 (in million tons), Statista, 2022.
- 8 North America, Polycarbonate For Electrical And Electronics Market Size, Share & Trends Analysis Report By End Use (IT Electronics, Electrical Enclosures), By Country (Canada, U.S.), And Segment Forecasts, 2021 2028, *Grand View Research*, 2021.

- 9 K. Schwartz, Polycarbonates in Construction, Performance Plastics Association (IAPD), 2015.
- 10 T. Hotaka, F. Kondo, R. Niimi, F. Togashi and Y. Morita, Polym. J., 2019, 51, 1249–1263.
- 11 Automotive Polycarbonate Glazing Market Global Industry Analysis, Size, Share, Growth, Trends, and Forecast, 2019–2027, ResearchAndMarkets.com, New York, 2019.
- 12 H. Abramowitz, T. Hentea, Y. Kin and Y. Xu, Ageing of Materials and Methods for the Assessment of Lifetimes of Engineering Plant Cape '97, 1997, pp. 309-317.
- 13 H. de Brouwer, J. van den Bogerd and J. Hoover, *Eur. Polym. J.*, 2015, 71, 558–566.
- 14 M. Scharfenberg, J. Hilf and H. Frey, *Adv. Funct. Mater.*, 2018, 28, 1704302.
- 15 E. Bormashenko, R. Pogreb, O. Stanevsky, Y. Bormashenko, Y. Socol and O. Gendelman, *Polym. Adv. Technol.*, 2005, 16, 299–304.
- 16 G. Gomez-Gras, M. D. Abad and M. A. Perez, *Polymers*, 2021, 13, 3669.
- 17 X. J. Bai, D. H. Isaac and K. Smith, *Polym. Eng. Sci.*, 2007, 47, 120–130.
- 18 L. Delva, K. Ragaert, J. Degrieck and L. Cardon, *Polymers*, 2014, 6, 2912–2927.
- 19 F. Elmaghor, L. Y. Zhang, R. Fan and H. Q. Li, *Polymer*, 2004, 45, 6719–6724.
- 20 W. B. Ding, J. Liang and L. L. Anderson, *Energy Fuels*, 1997, **11**, 1219–1224.
- 21 K. Ragaert, L. Delva and K. Van Geem, *J. Waste Manage.*, 2017, **69**, 24–58.
- 22 M. H. Zeng, Y. H. Lee, G. Strong, A. M. LaPointe, A. L. Kocen, Z. Q. Qu, G. W. Coates, S. L. Scott and M. M. Abu-Omar, ACS Sustainable Chem. Eng., 2021, 9, 13926–13936.
- 23 G. Celik, R. M. Kennedy, R. A. Hackler, M. Ferrandon, A. Tennakoon, S. Patnaik, A. M. LaPointe, S. C. Ammal, A. Heyden, F. A. Perras, M. Pruski, S. L. Scott, K. R. Poeppelmeier, A. D. Sadow and M. Delferro, ACS Cent. Sci., 2019, 5, 1795–1803.
- 24 F. Zhang, M. H. Zeng, R. D. Yappert, J. K. Sun, Y. H. Lee, A. M. LaPointe, B. Peters, M. M. Abu-Omar and S. L. Scott, *Science*, 2020, 370, 437–441.
- 25 B. A. Abel, R. L. Snyder and G. W. Coates, *Science*, 2021, 373, 783–789.
- 26 Z. Xu, F. Pan, M. Sun, J. Xu, N. E. Munyaneza, Z. L. Croft, G. Cai and G. Liu, *Proc. Natl. Acad. Sci. U. S. A.*, 2022, 119, e2203346119.
- 27 A. Rahimi and J. M. Garcia, Nat. Rev. Chem., 2017, 1, 0046.
- 28 I. Vollmer, M. J. F. Jenks, M. C. P. Roelands, R. J. White, T. van Harmelen, P. de Wild, G. P. van der Laan, F. Meirer, J. T. F. Keurentjes and B. M. Weckhuysen, *Angew. Chem.*, *Int. Ed.*, 2020, 59, 15402–15423.
- 29 H. Zhou, Y. Ren, Z. H. Li, M. Xu, Y. Wang, R. X. Ge, X. G. Kong, L. R. Zheng and H. H. Duan, *Nat. Commun.*, 2021, 12, 4679.
- 30 L. T. J. Korley, T. H. Epps, B. A. Helms and A. J. Ryan, *Science*, 2021, **373**, 66–69.

- 31 T. Yoshioka, K. Sugawara, T. Mizoguchi and A. Okuwaki, *Chem. Lett.*, 2005, **34**, 282–283.
- 32 G. D. Cooper and B. Williams, *J. Org. Chem.*, 1962, 27, 3717–3720.
- 33 E. Quaranta, Appl. Catal., B, 2017, 206, 233-241.
- 34 H. Tagaya, K. Katoh, J. Kadokawa and K. Chiba, *Polym. Degrad. Stab.*, 1999, **64**, 289–292.
- 35 G. Grause, R. Karrbrant, T. Kameda and T. Yoshioka, *Ind. Eng. Chem. Res.*, 2014, **53**, 4215–4223.
- 36 G. O. Jones, A. Yuen, R. J. Wojtecki, J. L. Hedrick and J. M. Garcia, *Proc. Natl. Acad. Sci. U. S. A.*, 2016, 113, 7722– 7726.
- 37 F. Iannone, M. Casiello, A. Monopoli, P. Cotugno, M. C. Sportelli, R. A. Picca, N. Cioffi, M. M. Dell'Anna and A. Nacci, J. Mol. Catal. A: Chem., 2017, 426, 107–116.
- 38 A. Ikeda, K. Katoh and H. Tagaya, *J. Mater. Sci.*, 2008, 43, 2437–2441.
- 39 G. Grause, K. Sugawara, T. Mizoguchi and T. Yoshioka, *Polym. Degrad. Stab.*, 2009, **94**, 1119–1124.
- 40 M. Watanabe, Y. Matsuo, T. Matsushita, H. Inomata, T. Miyake and K. Hironaka, *Polym. Degrad. Stab.*, 2009, 94, 2157–2162.
- 41 C. Puglisi, L. Sturiale and G. Montaudo, *Macromolecules*, 1999, 32, 2194–2203.
- 42 M. Day, J. D. Cooney, C. Touchette-Barrette and S. E. Sheehan, *J. Anal. Appl. Pyrolysis*, 1999, 52, 199–224.
- 43 B. N. Jang and C. A. Wilkie, *Polym. Degrad. Stab.*, 2004, 86, 419–430.
- 44 L. C. Hu, A. Oku and E. Yamada, *Polymer*, 1998, 39, 3841-3845.
- 45 A. Oku, S. Tanaka and S. Hata, *Polymer*, 2000, 41, 6749–6753.
- 46 D. Kim, B. K. Kim, Y. M. Cho, M. Han and B. S. Kim, *Ind. Eng. Chem. Res.*, 2009, 48, 685–691.
- 47 E. Quaranta, C. C. Minischetti and G. Tartaro, *ACS Omega*, 2018, 3, 7261–7268.
- 48 R. Arai, K. Zenda, K. Hatakeyama, K. Yui and T. Funazukuri, *Chem. Eng. Sci.*, 2010, **65**, 36–41.
- 49 S. Hata, H. Goto, E. Yamada and A. Oku, *Polymer*, 2002, **43**, 2109–2116.
- 50 S. Westhues, J. Idel and J. Klankermayer, *Sci. Adv.*, 2018, 4, eaat 9669.
- 51 M. Diepens and P. Gijsman, *Polym. Degrad. Stab.*, 2007, **92**, 397–406.
- 52 J. E. Pickett, Polym. Degrad. Stab., 2011, 96, 2253-2265.
- 53 G. Gryn'ova, J. L. Hodgson and M. L. Coote, *Org. Biomol. Chem.*, 2011, **9**, 480–490.
- 54 L. M. Smith, H. M. Aitken and M. L. Coote, *Acc. Chem. Res.*, 2018, **51**, 2006–2013.
- 55 J. L. Bolland, Proc. R. Soc. London, Ser. A, 1946, 186, 218-236.
- 56 J. L. Bolland and G. Gee, *Trans. Faraday Soc.*, 1946, 42, 236–243.
- 57 J. L. Bolland and G. Gee, *Trans. Faraday Soc.*, 1946, **42**, 244–252
- 58 J. L. Bolland and P. Tenhave, *Trans. Faraday Soc.*, 1947, 43, 201–210.
- 59 J. L. Bolland, Trans. Faraday Soc., 1948, 44, 669-677.
- 60 J. L. Bolland, Trans. Faraday Soc., 1950, 46, 358-368.
- 61 D. Graebling, *Macromolecules*, 2002, **35**, 4602–4610.

- 62 E. Borsig, A. Fiedlerova, L. Rychla, M. Lazar, M. Ratzsch and G. Haudel, *J. Appl. Polym. Sci.*, 1989, 37, 467–478.
- 63 A. François-Heude, E. Richaud, E. Desnoux and X. Colin, J. Photochem. Photobiol., A, 2015, 296, 48-65.
- 64 V. J. Triacca, P. E. Gloor, S. Zhu, A. N. Hrymak and A. E. Hamielec, *Polym. Eng. Sci.*, 1993, 33, 445–454.
- 65 Y. Ahn, G. Roma and X. Colin, *Macromolecules*, 2022, 55, 8676–8684.
- 66 C. L. Opstad, T. B. Melo, H. R. Sliwka and V. Partali, Tetrahedron, 2009, 65, 7616–7619.
- 67 Y. C. Zhu, Z. Y. Zhang, R. Jin, J. Z. Liu, G. Q. Liu, B. Han and N. Jiao, *Angew. Chem., Int. Ed.*, 2020, **59**, 19851–19856.
- 68 R. Herscu-Kluska, A. Masarwa, M. Saphier, H. Cohen and D. Meyerstein, *Chem. Eur. J.*, 2008, **14**, 5880–5889.
- 69 X. Jiang, C. Wang, Y. W. Wei, D. Xue, Z. T. Liu and J. L. Xiao, *Chem. Eur. J.*, 2014, **20**, 58–63.
- 70 J. Jia, Q. Jiang, A. Zhao, B. Xu, Q. Liu, W. P. Luo and C. C. Guo, *Synthesis*, 2016, 48, 421–428.
- 71 M. K. Eberhardt and R. Colina, J. Org. Chem., 1988, 53, 1071–1074.
- 72 G. A. Russell and S. A. Weiner, *J. Org. Chem.*, 1966, 31, 248–251.
- 73 M. J. Burkitt and R. P. Mason, *Proc. Natl. Acad. Sci. U. S. A.*, 1991, **88**, 8440–8444.
- 74 L. M. Bellotindos, M. H. Lu, T. Methatham and M. C. Lu, *Environ. Sci. Pollut. Res.*, 2014, **21**, 14158–14165.
- 75 J. F. Guan, J. Peng and X. Y. Jin, *Anal. Methods*, 2015, 7, 5454–5461.
- 76 Y. X. Xie, Y. Qian, Z. X. Li, Z. C. Liang, W. F. Liu, D. J. Yang and X. Q. Qiu, ACS Sustainable Chem. Eng., 2021, 9, 6479– 6488.
- 77 Y. X. Xie, C. C. Gan, Z. X. Li, W. F. Liu, D. J. Yang and X. Q. Qiu, *ACS Biomater. Sci. Eng.*, 2022, **8**, 560–569.
- 78 Z. J. Yang, Y. Cao, J. Li, M. M. Lu, Z. K. Jiang and X. Y. Hu, *ACS Appl. Mater. Interfaces*, 2016, **8**, 12031–12038.
- 79 P. L. Li, M. Wang, M. Z. Jiang, W. J. Lai, J. J. Li, K. L. Liu, H. L. Li and C. L. Hong, New J. Chem., 2022, 46, 13963– 13970.
- 80 M. Q. Sun, N. Kreis, K. X. Chen, X. Q. Fu, S. Guo and H. Wang, *Chem. Mater.*, 2021, 33, 8546–8558.
- 81 M. Q. Sun, X. Q. Fu, K. X. Chen and H. Wang, *ACS Appl. Mater. Interfaces*, 2020, **12**, 46146–46161.
- 82 H. L. Cao, X. F. Qian, C. Wang, X. D. Ma, J. Yin and Z. K. Zhu, *J. Am. Chem. Soc.*, 2005, **127**, 16024–16025.
- 83 Q. W. Tian, M. H. Tang, Y. G. Sun, R. J. Zou, Z. G. Chen, M. F. Zhu, S. P. Yang, J. L. Wang, J. H. Wang and J. Q. Hu, *Adv. Mater.*, 2011, 23, 3542–3547.
- 84 G. K. S. Prakash, H. Vaghoo, C. Panja, V. Surampudi, R. Kultyshev, T. Mathew and G. A. Olah, *Proc. Natl. Acad. Sci. U. S. A.*, 2007, **104**, 3026–3030.
- 85 M. M. Heravi, M. Ghavidel and L. Mohammadkhani, *RSC Adv.*, 2018, **8**, 27832–27862.
- 86 M. A. Krestyaninov, M. G. Kiselev and L. P. Safonova, *Russ. J. Phys. Chem.*, 2015, **89**, 608–615.
- 87 R. H. Boyd, in *Thermal Stability of Polymers*, ed. R. T. Conley, Marcel Dekker Inc., New York, 1970, vol. 1.